Highly Thermally Conductive Papers with Percolative Layered Boron Nitride Nanosheets

Hongli Zhu,[†] Yuanyuan Li,[†] Zhiqiang Fang,[†] Jiajun Xu,[‡] Fangyu Cao,[‡] Jiayu Wan,[†] Colin Preston,[†] Bao Yang,[‡,*] and Liangbing Hu[‡,*]

[†]Department of Materials Science and Engineering, University of Maryland, College Park, Maryland 20742, United States and [‡]Department of Mechanical Engineering, University of Maryland, College Park, Maryland 20742, United States

ABSTRACT In this work, we report a dielectric nanocomposite paper with layered boron nitride (BN) nanosheets wired by one-dimensional (1D) nanofibrillated cellulose (NFC) that has superior thermal and mechanical properties. These nanocomposite papers are fabricated from a filtration of BN and NFC suspensions, in which NFC is used as a stabilizer to stabilize BN nanosheets. In these nanocomposite papers, two-dimensional (2D) nanosheets form a thermally conductive network, while 1D NFC provides mechanical strength. A high thermal conductivity has been achieved along the BN paper surface (up to 145.7 W/m K for 50 wt % of BN), which is an order of magnitude higher than that in randomly distributed BN nanosheet composites and is even comparable to the thermal conductivity of aluminum alloys. Such a high thermal conductivity is mainly attributed to the structural alignment within the BN nanosheet papers; the effects of the interfacial thermal contact resistance are minimized by the fact that the heat transfer is in the direction parallel to the interface between BN nanosheets and that a large contact area occurs between BN nanosheets.

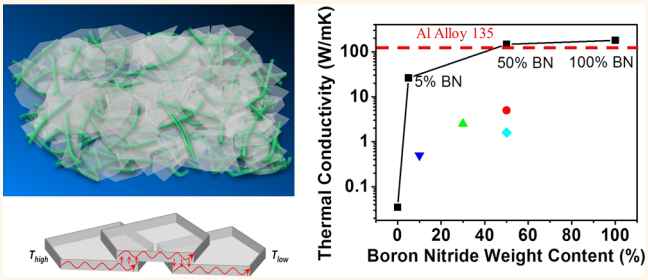

KEYWORDS: nanocomposite paper · boron nitride nanosheets · thermal conductivity · percolative network · optical transparence · nanofibrillated cellulose

Small yet powerful cockpit microelectronics found in military, automotive, and aerospace products generate intense heat that causes device failure; thus, there is a need to address thermal dissipation in the device designs. The current materials for conducting heat in aerospace devices are aluminum alloys, which typically have a thermal conductivity of 130 W/mK; however, the density of aluminum alloys makes them unfavorable for aerospace applications. Recent reports demonstrate lightweight nanocomposites incorporated with thermally conductive nanomaterials, such as carbon nanotubes (CNTs), graphene, and boron nitride (BN) nanosheets.[1−7] These individual nanomaterials have ultrahigh thermal conductivity due to limited phonon scattering and high phonon velocity. The thermal conductivity is 3500 W/mK for individual single walled carbon nanotubes at room temperature,[8] 2000−4000 W/mK for monolayer graphene,[9] and 2000 W/mK for BN.[10] Unlike CNTs or graphene, BN is an electrical insulator with a dielectric constant of 3−4,[11] and thus has applications in thermal management of high power electronics and displays that are not possible for CNTs and graphene. The thermal conductivity of conventional BN nanocomposites, however, is only around 5 W/mK.[7,12,13] A recent study demonstrated polyhedral oligosilsesquioxane modified boron nitride nanotube (BNNT) based epoxy nanocomposite has a thermal conductivity of 2.7 W/mK with 30 wt % of BNNT at 25 °C.[14] The low thermal conductivity is due to the random distribution of BNNTs in the composite, and the thermal insulating epoxy further hinders phonon transport. Note that the BN based films are thermally conductive and electrically insulating, which is promising for dielectric applications in complex and powerful microelectronics or integrated devices.

In particular for portable flexible microelectronic applications, substrates such as paper, glass, and plastic all have a very low thermal conductivity. For example,

* Address correspondence to binghu@umd.edu, baoyang@umd.edu.

Received for review January 8, 2014 and accepted March 6, 2014.

Published online March 06, 2014
10.1021/nn500134m

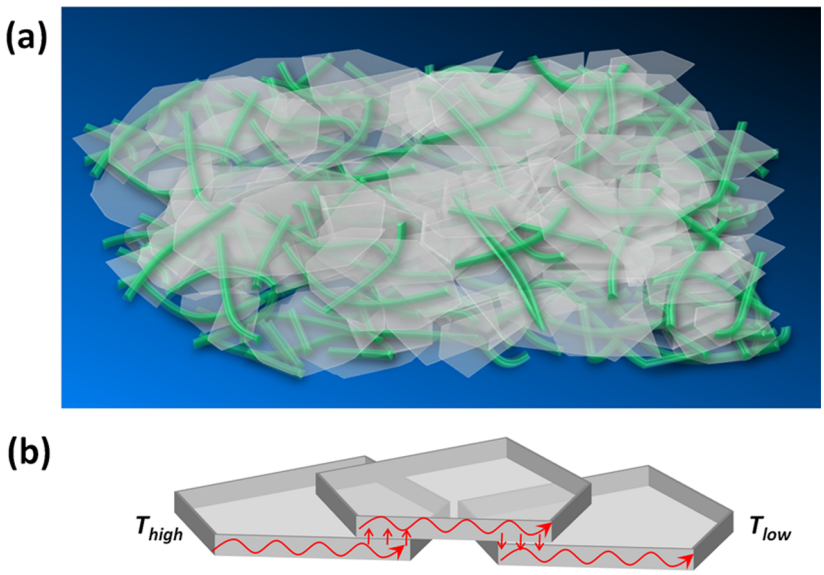

Figure 1. (a) Schematic to show the structure of cellulose nanofiber with layered boron nitride nanosheets to conduct heat in the horizontal plane direction. (b) A schematic to show how phonons are transmitted between BN layers.

conventional paper has a very low thermal conductivity of 0.03 W/mK, while that of plastic is 0.23 W/mK.[15,16] There is an urgent need to increase the thermal conductivity of these substrates for flexible electronic devices. In this study, we designed a novel structural nanocomposite paper based on 2D BN and 1D NFC, which is fabricated with a standard filtration papermaking process. 2D BN nanosheets are aligned in the planar direction, which can maximize the overlapping area, reduce percolation threshold, and decrease thermal contact resistance. Novel NFC not only serves as a stabilizer, but more importantly, it links the nanosheets together to enhance mechanical strength in the nanosheet paper. The dielectric constant of naocellulose presented in this work is 4.5.[17] The single cellulose microfibril has an elastic modulus in the axial direction as high as 145 GPa,[18] which dramatically increases the mechanical strength of the hybrid paper. Since the NFC has a 1D nanofiber structure as opposed to other polymers, they will form less insulating contacts between BN sheets. The contact area between the layered BN nanosheets is therefore increased. We demonstrate that BN can dramatically increase the thermal conductivity of NFC based transparent nanopaper. Incorporation of 5% BN can multiply the thermal conductivity by 1000 times. A freestanding and flexible film with a thermal conductivity of up to 150 W/mK is achieved, which is an order of magnitude higher than that for randomly distributed BN nanosheet composites and is even comparable to the thermal conductivity of aluminum alloys. In addition to freestanding films, we also demonstrated that the stable BN/NFC ink can be conformably coated on the paper, textile, and electronic circuit surface to make low-cost, lightweight, and thermally conductive multifunctional materials.

RESULTS AND DISCUSSION

A schematic of the BN nanosheet composite paper configuration is shown in Figure 1a,b. In this design, BN nanosheets provide a thermal transport path while NFC wires can enhance the mechanical strength of BN paper. As shown in Figure 1b, the BN nanosheets are well aligned in the direction along the paper surface. Large contact area is achieved between BN nanosheets, and therefore, the thermal contact resistance is minimized when heat transfers along the paper surface. Unlike a traditional polymer-like resin or polymethyl methacrylate (PMMA), NFC fibers do not form thermally insulating contacts between the BN flakes. When BN is less than 5 wt %, the composite film is highly optically transparent, allowing it to be used as a substrate for transparent flexible electronics that is capable of dissipating heat.

Large quantities of 2D BN nanosheets as shown in Figure 2a were exfoliated by sonicating commercial hexagonal BN (HBN) micropowder in isopropanol alcohol (IPA).[19] The obtained BN thickness varies from a few to several layers with a typical lateral size of 200−3000 nm, Figure 2b,c and Supporting Information, Figures S1 and S2. Figure 2c illustrates a 3 nm thick BN film (less than 10 layers). Cellulose is an organic compound composed with D-glucose *via* β (1→4) linkage that is nearly inexhaustible with outstanding biodegradability and biocompatibility.[20] The 1D NFC was disintegrated from the wood fibers with a pretreatment of NaBr/NaClO/TEMPO (2,2,6,6-tetramethylpiperidine-1-oxyl) and homogenized with a microfluidizer.[21,22] After a TEMPO oxidation, an abundance of ionized carboxyl groups ($-COO^-$) were introduced onto the surface of the NFC. The repulsive forces generated by surface carboxyl groups make NFC stable

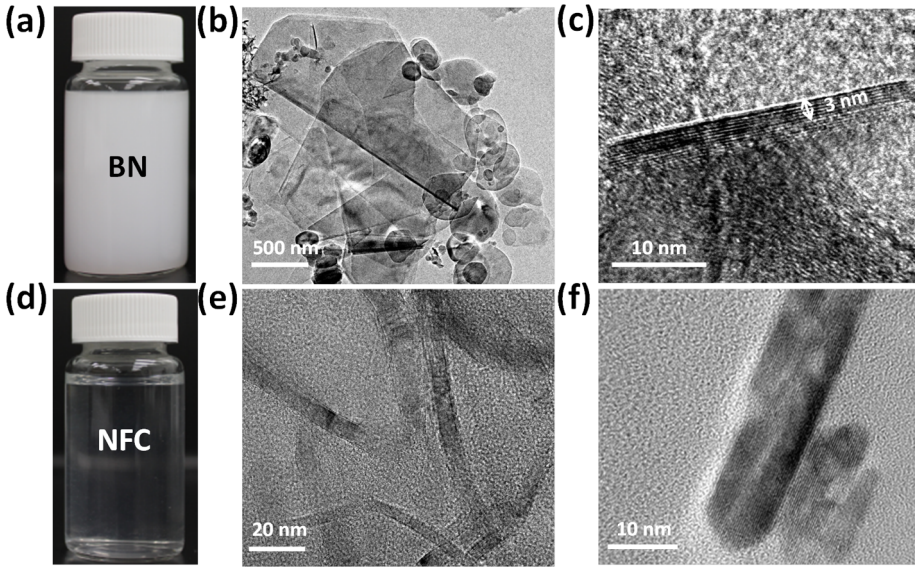

Figure 2. (a) Image of BN dispersed in IPA. (b) TEM image of BN nanoplates. (c) TEM image showing the edge of BN nanosheets. (d) Image of transparent nanocellulose fibers in water. (e) TEM image of nanocellulose fiber. (f) High resolution TEM image to show the crystalline pattern of nanocellulose fiber.

in water without forming aggregates. Additionally, the resulting NFC water solution is transparent, as shown in Figure 2d. Figure 2e shows that the diameter of the NFC is around 5−10 nm. The NFC also possesses 80−90% crystallinity that is clearly depicted in the image of high-resolution transmission electron microscopy (HRTEM) in Figure 2f.

A BN solution is compatible with a NFC solution without agglomerating. The hybrid solutions with 5 wt % BN (left) and 50 wt % BN (right) are uniform and stable after 3 months, as shown in Figure 3a. In the hybrid solution, the NFC acts as a stabilizer for BN. After exfoliation by sonication, hydroxyl groups and amino groups are formed on the BN edges due to the hydrolysis.[13,23] NFC easily absorbs onto BN nanosheets due to the abundant surface hydroxyl groups. The repulsive forces generated by surface carboxyl groups between NFC fibers provide stability in the hybrid solution. The well dispersed stable solution is critical to obtain a uniform freestanding nanocomposite film without defects, which is important to achieve both excellent mechanical strength and phonon thermal conductivity. The 25−30 μm thick nanocomposite films with different ratios of BN were fabricated through a simple and scalable paper-making process. Figure 3b,c shows the films made from 5 wt % BN and 50 wt % BN, respectively. As shown in Figure 3b, the letters and pattern beneath the film are clearly visible. The 5% BN film has 67% transmittance at 550 nm wavelength (Figure 3d). With a higher BN ratio, the film is opaque with only 9% transmittance at 550 nm wavelength and 86% whiteness. Paper with tailored optical properties can be used for different applications; for example, cellulose paper with 5% BN incorporation can be used as transparent substrate to replace plastic for flexible electronics applications. Cellulose paper with a much higher BN content shows excellent whiteness and potentially low IR and microwave absorption, which can be applied as ideal thermal conductors for military applications.

Figure 3e shows the thermal conductivity *vs* weight content of BN. The pure cellulose has a poor thermal conductivity of 0.035 W/mK. With only 5% BN loading, the thermal conductivity is increased from 0.035 W/mK to 26.2 W/mK, which significantly exceeds the conductivity of the composite made from 10 wt % BN nanotube (BNNT)/resin, 0.7 W/mK at 25 °C.[14] The thermal conductivity of the film increased to 145.7 W/mK with 50% BN, which is ~30 times higher than the conductivity of the composites reported in literature with the similar BN weight content,[12−14,24] and comparable with conventional airspace materials such as aluminum alloy.

To understand thermal transport in the BN nanosheet composite paper, a 3-dimensional numerical thermal model was developed using the commercial finite element software ANSYS. The simulation results are shown in Figure 3f, in which the BN nanosheets are assumed to have a thermal conductivity of 1000 W/mK. It can be seen that the effective thermal conductivity of the composite paper changes by a factor of 33 when the thermal interfacial resistance varies by 5 orders of magnitude in the nanocomposite papers with 70 vol % of BN nanosheets. In this layered composite paper, the effective thermal conductivity becomes much less sensitive to interfacial thermal resistance compared to conventional spherical particle composites. This is due to the large contact area between these nanosheets. When heat transfer is in the direction parallel to the BN nanosheets, the effects of interfacial thermal contact resistance can be

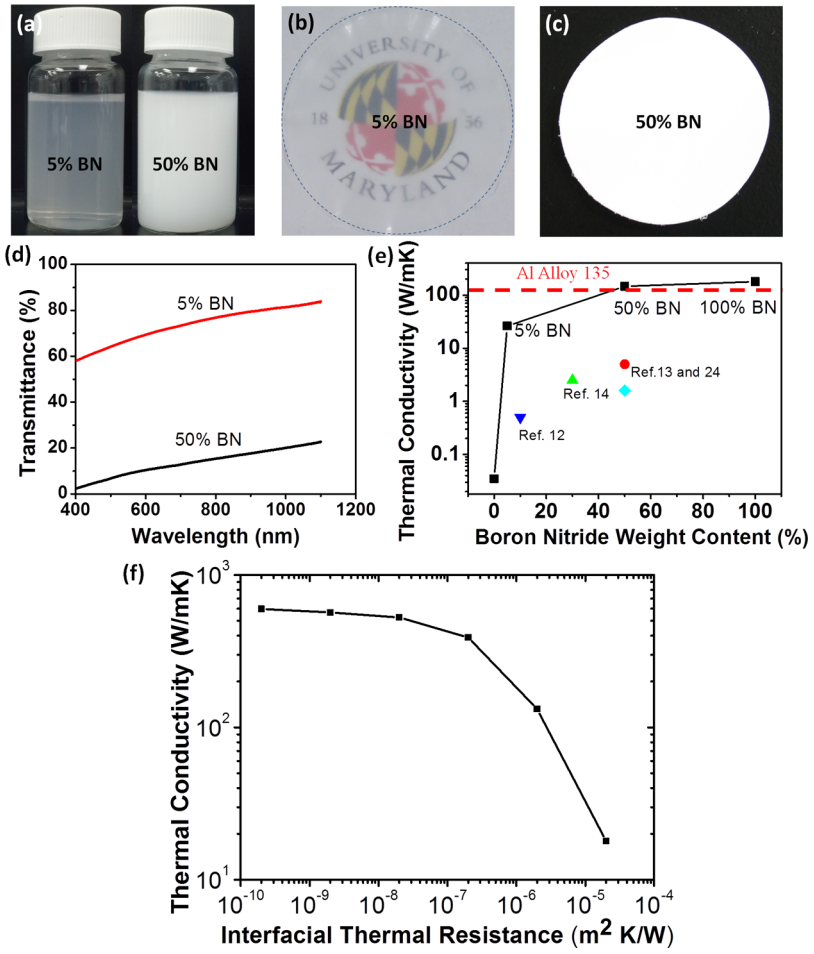

Figure 3. (a) An image of the stable mixture with 5 wt % BN and 95 wt % NFC in water at a concentration of 1.9 and 1.6 mg/mL, respectively. (b) Image of transparent and thermal conductive film with 5 wt % BN. (Image credit: University of Maryland seal. Trademark of the University of Maryland and used with permission.) (c) Image of white film with 50 wt % BN. (d) Transmittance of BN/NFC composite film with 5 and 50 wt % of BN. (e) Thermal conductivity *vs* BN content in BN/NFC composite. BN nanosheets largely improve the thermal conductivity, with a value of 145.7 W/mK with 50 wt % BN. (f) Numeric simulation results of effective thermal conductivity of BN nanosheet composite paper as function of the interfacial thermal resistance.

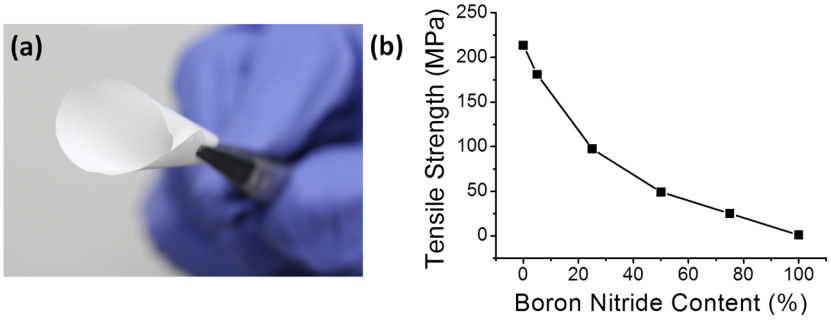

Figure 4. (a) A picture of BN film to show its flexibility. (b) Tensile strength *vs* BN content in the composite paper.

minimized, and therefore a very large thermal conductivity can be achieved in this direction.[25−28]

A freestanding film with good thermal conductivity, whiteness, or transmittance is important for advanced electronics. In addition to good thermal conductivity, excellent whiteness or good optical transmittance, BN/NFC hybrid films also show excellent mechanical flexibility and strength. As shown in Figure 4a, the nanocomposite film has good flexibility. The influence of BN loading on the tensile strength is compared in Figure 4b. The sample with 5% BN has a tensile strength of 181 MPa, and the tensile strength reduced with an increase of BN content. Note that pure BN film has weak strength and it is difficult to peel the film off from the filter paper as a freestanding film, while the NFC has excellent mechanical strength.

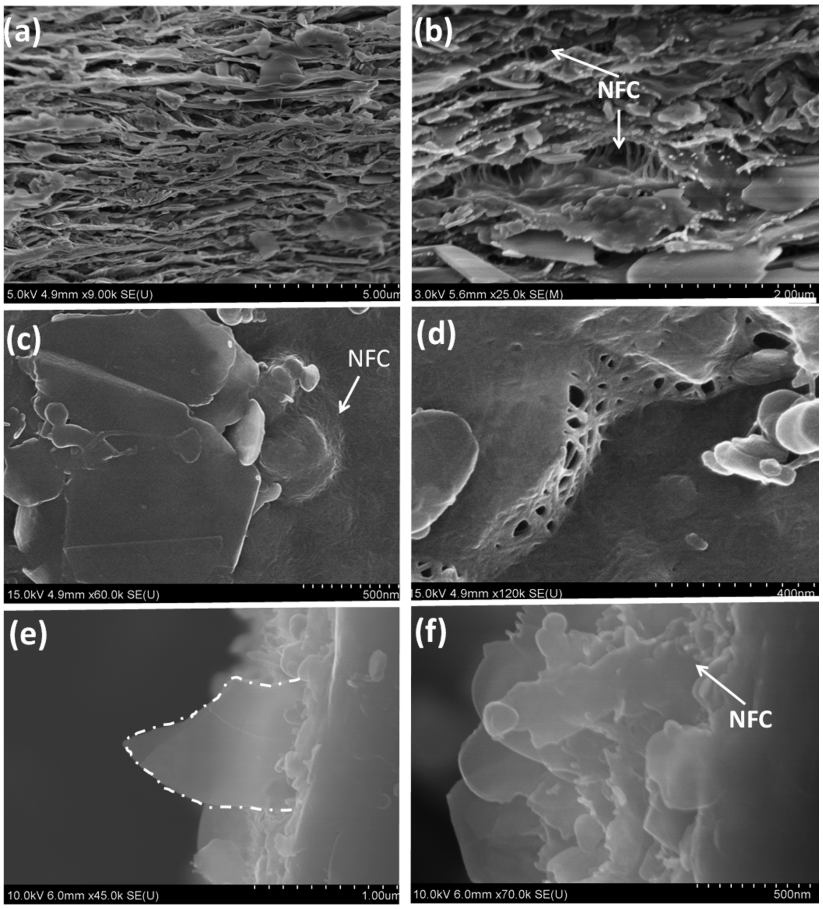

Figure 5. (a) SEM cross section image, and (b) a magnified image of the nanocomposite film with 50 wt % BN and 50 wt % NFC, which shows a well-defined layered structure. (c) SEM surface morphology image, and (d) a magnified image of the nanocomposite film with 50 wt % BN and 50 wt % NFC. (e) SEM cross section image, and (f) a magnified image of the fracture surface after force loading for the tensile strength test.

The cellulose microfibril has a Young's modulus up to 145 GPa.[29,30] In the hybrid film, the 1D NFC fibers enhance the strength of the composite film as a glue by wrapping the 2D plates together. Meanwhile, the edge of the BN platelets have functional groups such as hydroxyl groups (−OH) and amino groups ($-NH_2$).[13] The nanocellulose fiber surface has huge amount of hydroxyl groups (−OH) and carboxyl groups (−COOH). On the basis of this, we expect there is hydrobonding between the NFC and BN. The density of the NFC/BN hybrid film is in the range of 1.2−1.5 g/cm^3, which is 50% lighter than aluminum (2.7 g/cm^3). A strong and lightweight nanocomposite film with superior thermal conductivity promises huge potential aerospace applications.

To shed light on the high thermal conductivity and mechanical strength, the representative scanning electron microscope (SEM) micrographs of a cross section of 50% BN/50%NFC film is shown in Figure 5a. The image shows that the 2D planes are tightly stacked and the layered structure is well preserved in the film cross section. This film has a high thermal conductivity of 145.7 W/mK. The tightly packed layered structure plays a key role in the efficient phonon transfer between two nanosheets. Rather than mixing the components in a compounder and hot pressed under high pressure,[24] the oriented layered structure is formed in the filtration process. The 2D nanosheets mixed with 1D nanofibers is also an effective architecture to preserve the planar network rather than gluing everything together into a solid structure. The compounding of polymers, including polyimide,[13] epoxy,[14] PMMA,[12] polyvinyl alcohol-(PVA),[7] and styrene-ethylene-butylene-styrene terpolymer (SEBS)/poly(ethylene-*co*-vinyl acetate) (EVA) blends, are viscous bulky polymers.[24] These viscous polymers do not allow the formation of layered structures for BN sheets.[24] The unique layered structure that incorporate fibers as glue for the 2D nanosheets dramatically increases the thermal conductivity. In the magnified image of Figure 5b, the NFC is clearly observed between the layered nanosheets.

Figure 5c illustrates a SEM image of the 50% BN/50% NFC film surface in which a large BN plate is clearly observed. The NFC fibers are also observable around the BN plate. Figure 5d illuminates the 2D BN sheets linked by 1D fibers to form a strong network, and that they are tightly packed into a layered structure. All these structures adequately explain the excellent thermal conductivity of this tightly packed and layered material.

TABLE 1. Comparison of Thermal Conductivity and Tensile Strength between Our BN Paper with the Best Data from Literature[5,33,7,12−14,24,33,4] [a]

	thermal conductivity K (W/mK)	electrical conductivity	tensile strength	reference
Single BN nanosheet	2000	No	102 GPa	10
Single Graphene Sheet	2000−4000	Yes	110 GPa	31, 32
BN nanocomposite	≤20	No	120 MPa	7, 13
Graphene nanocomposite	≤80	Yes	200 MPa	5, 33, 34
2D layered structure	150−180	No	180 MPa	This work

[a] Note that the electrical insulating nature of BN paper can open applications that are impossible for graphene-based composites.

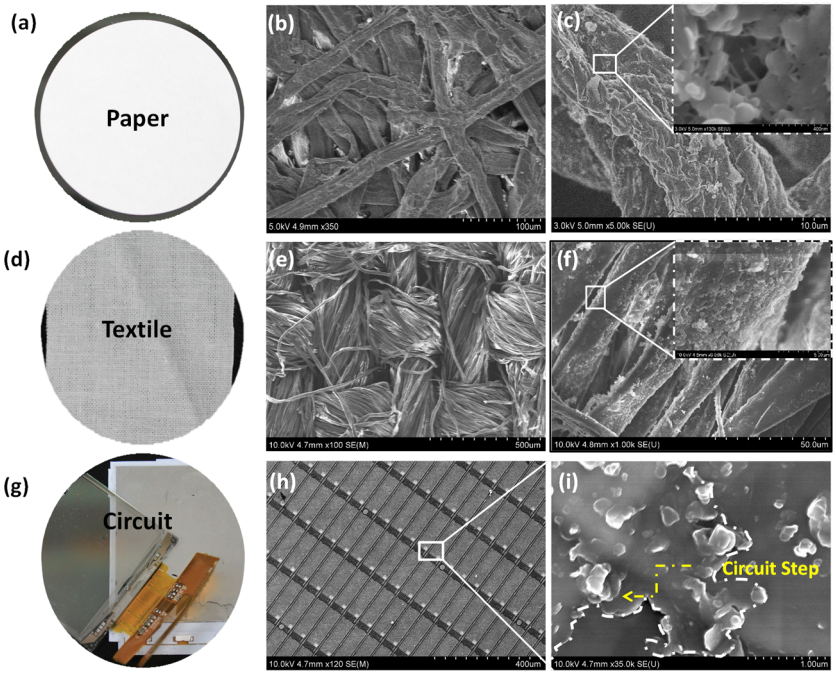

Figure 6. A stable BN ink is applied for coating on different substrates: (a) an image of thermally conductive paper coated with BN/NFC ink. The thermal conductive paper has excellent whiteness. (b) SEM image shows the 3D fibers network structure of paper. (c) SEM image of the fiber surface morphology with an inset magnified image to show the 1D NFC fibers gluing 2D BN plate together. (d) An image of thermal conductive textile coated with BN. Textile fiber morphological SEM images are shown in (e) and (f). (g) An image of an display color filter coated with BN flakes. Circuit surface morphological SEM images are shown in (h) and (i).

Figure 5e,f demonstrate the fracture surface of the film after force loading for the tensile strength test in which a large plate of BN is clearly broken. In addition to the 2D plate, the 1D fibers are also clearly defined in Figure 5f.

It is worthwhile to compare our performance achieved with BN nanosheets to graphene-based nanocomposites due to their structural similarity. Note that graphene is electrically conductive but BN is electrically insulating, and thus they are useful for very different applications. Extremely high thermal conductivities are reported for monolayer graphene and BN, with a value of (2.6 ± 0.9) to $(3.1 \pm 1.0) \times 10^3$ W/mK at 350 K and 2000 W/mK, respectively.[10,31] Meanwhile, excellent mechanical properties are reported for both graphene and BN, with a tensile strength of 110 and 102 GPa, respectively.[10,32] 2D BN and graphene are consequently excellent additives in nanocomposites to achieve both high thermal conductivity and mechanical strength. Table 1 summarizes the best values for nanocomposites with percolative BN and graphene flakes. Our unique layered structure wired together by 1D NFC fibers leads to the best combined performance in thermal conductivity and mechanical strength due to the layered structure with in-plane coupling.

The stable and scalable ink used to fabricate the above-mentioned paper can be applied to functionalize thermal isolating substrates, such as paper, fabric, and glass. Figure 6a is an image of paper coated with the ink (75 wt % BN and 25 wt % NFC in water at the concentration of 1.6 mg/mL). The obtained thermal conductive paper is foldable, lightweight, and stable. After the additional BN coating, the paper keeps the original appearance with a favorable whiteness, which is dramatically different than a graphene coating. Figure 6b shows the thermal conductive paper surface morphology. A magnified image of the fiber surface is illustrated in Figure 6c. The 1D NFC fibers link the 2D flakes together, functioning as glue; therefore,

the obtained thermally conductive paper has high mechanical stability. Figure 6d demonstrates that a similar process may be applied to other substrates, such as textiles. A conformal layer of BN was coated on the textile fiber surface as shown in Figure 6e,f. The resulting BN layer is expected to have high thermal conductivity and gas barrier properties; therefore the thermally conductive textile can be potentially applied as a fire retardant material. The heat dissipation is important for small electronics. We coated one layer of BN ink on the surface of cellphone display color filter *via* a facial dipping process, as seen in Figure 6g,h. As shown in the magnified image in Figure 6i and Supporting Information Figure S3, the flexible BN plates cover the steps in the circuit perfectly. The extremely conformal coating with BN-NFC hybrid ink may provide an effective way to remove heat from these substrates, which enables a range of device applications.

CONCLUSION

In summary, we demonstrate nanocomposites paper fabricated from 2D BN nanosheets and 1D NFC based inks where NFC functions as a stabilizer to stabilize BN. The resulting film has superior combined thermal conductivity and mechanical strength, which is due to the intrinsic layered structure with excellent in-plane coupling between BN nanoplates wired by 1D NFCs. The transmittance and whiteness of the paper can be tuned by adjusting the BN content. The composite paper containing 50 wt % BN has a high thermal conductivity of 145.7 W/mK, which is approximately ten times better than any other BN based composite and is comparable to aluminum alloys. Intrinsically insulating BN-NFC hybrid paper with high thermal conductivity can open applications that are impossible with other electrically conductive materials such as CNTs and graphene.

EXPERIMENTAL SECTION

Preparation of BN Ink Exfoliation and NFC Gel. BN micropowder was purchased from Graphene Supermarket, Inc. Commercial BN powder was dispersed in IPA with a concentration of 5 mg/mL. The dispersion was sonicated for 48 h in a sonic bath (FS 110D, Fisher Scientific). The dispersion was then centrifuged at 1000 rpm for 15 min and decanted immediately. The concentration of the obtained ink was 0.77 mg/mL. The NFC was disintegrated from wood pulp based on the method proposed in Zhu's paper.[21]

Transmission Electron Microscopy (TEM) JEOL JEM 2100 (Japan) performed at an accelerating voltage of 200 kV was employed for the BN and NFC morphology characterization.

Nanocomposite Film Fabrication and Characterization. The NFC was diluted to 0.2 wt % with deionized water in a glass flask and stirred for 30 min under magnetic stirrer. The BN suspension was then dropped into a NFC dispersion during the stirring. The mixture of BN and NFC was kept stirring for 10 min and placed in a bath sonification for 15 min to form uniform BN/NFC suspension. The prepared BN/NFC suspension was filtered with a Bucher funnel using a filter membrane (pore size: 0.65 μm, Millipore). The obtained wet film was placed between filter papers and dried at room temperature under mechanical pressing. The basic weight of BN/NFC film is around 40 g/m^2. The film morphology and thickness were tested with a Hitachi SU-70 field emission scanning electron microscopy (FESEM) with an accelerating voltage at 5−10 kV. The tensile strength of the BN paper was characterized by a dynamic mechanical analysis (DMA) machine (Q800) under tension film mode. During the extension process, the rate was 1%/min. Each sample was cut into a strip of 3 mm × 20 mm. The whiteness of the film was tested with YA-Z-48B Whiteness Meter (YQ-Z-48B) (Hangzhou Qingtong & Boke Automation Technology Co., Ltd.). The optical transmittance of the nanocomposite film was obtained with a UV−vis Spectrometer Lambda 35 (PerkInElmer), and the transmittance was measured between 1100 and 250 nm using a Shimadzu UV−vis spectrometer.

Thermal Conductivity Measurement. The thermal conductivity along the BN nanosheet papers was measured using the steady-state method, as shown in Supporting Information, Figure S4.[34,35] The nanosheet paper sample is about 8 mm wide and 30 mm long. A heat sink was attached one end of the paper sample, and the other end was connected to an electric heater. Two fine-gage, K-type thermocouples separated by a distance L were used to measure the temperature difference ΔT along the sample. The sample was placed in a vacuum chamber with heat shield to minimize the heat loss. When steady-state was reached, the thermal conductivity of the sample was determined by applying Fourier's law:

$$k = \frac{Q_S L}{A\Delta T} \quad (1)$$

where Q_S is the power flowing through the sample, L is the distance between the thermocouple leads, A is the cross section area of the sample through which the power flows, and ΔT is the temperature difference measured. If there is no heat loss, all the power supplied to the heater flows through the sample and into the heat sink; therefore, the heat flowing across any cross section would be constant. In real measurements, heat loss is inevitable through radiation, convection and heat conduction, so the power flowing through the sample Q_s can be written as

$$Q_S = Q_{in} - Q_{loss} \quad (2)$$

where Q_{loss} is the power lost by radiation, heat conduction through the connection leads, and convection. Calibration experiments are performed for Teflon film (k = 0.25 W/mK) and copper alloy 110 (k = 380 W/mK). The uncertainty of the thermal conductivity measurement along the film samples is about 10%.

Conflict of Interest: The authors declare no competing financial interest.

Acknowledgment. L. Hu acknowledges the support from DOD (Air Force of Scientific Research) Young Investigator Program (FA95501310143). B. Yang acknowledges the support from NSF (CBET 1232949). We acknowledge the support of the Maryland Nanocenter and its Fablab and its Nisplab. The Nisplab is supported in part by the NSF as a MRSEC shared experimental facility. We acknowledge Dr. Peter Kofinas for sharing DMA machine.

Supporting Information Available: BN thickness characterized with high resolution TEM (HRTEM); BN lateral dimension characterized with TEM; SEM image of circuit covered by BN; schematic illustration of the steady-state thermal conductivity method for measuring the thermal conductivity along the nanosheet paper samples. This material is available free of charge *via* the Internet at http://pubs.acs.org.

REFERENCES AND NOTES

1. Nan, C.-W.; Liu, G.; Lin, Y.; Li, M. Interface Effect on Thermal Conductivity of Carbon Nanotube Composites. *Appl. Phys. Lett.* **2004**, *85*, 3549–3551.
2. Kumari, L.; Zhang, T.; Du, G. H.; Li, W. Z.; Wang, Q. W.; Datye, A.; Wu, K. H. Thermal Properties of CNT-Alumina Nanocomposites. *Compos. Sci. Technol.* **2008**, *68*, 2178–2183.
3. Han, Z.; Fina, A. Thermal Conductivity of Carbon Nanotubes and Their Polymer Nanocomposites: A Review. *Prog. Polym. Sci.* **2011**, *36*, 914–944.
4. Wang, X. L.; Bai, H.; Yao, Z. Y.; Liu, A. R.; Shi, G. Q. Electrically Conductive and Mechanically Strong Biomimetic Chitosan/Reduced Graphene Oxide Composite Films. *J. Mater. Chem.* **2010**, *20*, 9032–9036.
5. Song, S. H.; Park, K. H.; Kim, B. H.; Choi, Y. W.; Jun, G. H.; Lee, D. J.; Kong, B.-S.; Paik, K.-W.; Jeon, S. Enhanced Thermal Conductivity of Epoxy−Graphene Composites by Using Non-Oxidized Graphene Flakes with Non-Covalent Functionalization. *Adv. Mater.* **2013**, *25*, 732–737.
6. Lee, J.-U.; Yoon, D.; Kim, H.; Lee, S. W.; Cheong, H. Thermal Conductivity of Suspended Pristine Graphene Measured by Raman Spectroscopy. *Phys. Rev. B* **2011**, *83*, 081419.
7. Song, W. L.; Wang, P.; Cao, L.; Anderson, A.; Meziani, M. J.; Farr, A. J.; Sun, Y. P. Polymer/Boron Nitride Nanocomposite Materials for Superior Thermal Transport Performance. *Angew. Chem., Int. Ed.* **2012**, *51*, 6498–6501.
8. Pop, E.; Mann, D.; Wang, Q.; Goodson, K.; Dai, H. Thermal Conductance of an Individual Single-Wall Carbon Nanotube above Room Temperature. *Nano Lett.* **2005**, *6*, 96–100.
9. Chen, S.; Moore, A. L.; Cai, W.; Suk, J. W.; An, J.; Mishra, C.; Amos, C.; Magnuson, C. W.; Kang, J.; Shi, L.; Ruoff, R. S. Raman Measurements of Thermal Transport in Suspended Monolayer Graphene of Variable Sizes in Vacuum and Gaseous Environments. *ACS Nano* **2010**, *5*, 321–328.
10. Lin, Y.; Connell, J. W. Advances in 2D Boron Nitride Nanostructures: Nanosheets, Nanoribbons, Nanomeshes, and Hybrids with Graphene. *Nanoscale* **2012**, *4*, 6908–6939.
11. Dean, C. R.; Young, A. F.; Meric, I.; Lee, C.; Wang, L.; Sorgenfrei, S.; Watanabe, K.; Taniguchi, T.; Kim, P.; Shepard, K. L.; Hone, J. Boron Nitride Substrates for High-Quality Graphene Electronics. *Nat. Nano* **2010**, *5*, 722–726.
12. Zhi, C. Y.; Bando, Y.; Wang, W. L. L.; Tang, C. C. C.; Kuwahara, H.; Golberg, D. Mechanical and Thermal Properties of Polymethyl Methacrylate-BN Nanotube Composites. *J. Nanomater.* **2008**, *642036*, 1–5.
13. Sato, K.; Horibe, H.; Shirai, T.; Hotta, Y.; Nakano, H.; Nagai, H.; Mitsuishi, K.; Watari, K. Thermally Conductive Composite Films of Hexagonal Boron Nitride and Polyimide with Affinity-Enhanced Interfaces. *J. Mater. Chem.* **2010**, *20*, 2749–2752.
14. Huang, X. Y.; Zhi, C. Y.; Jiang, P. K.; Golberg, D.; Bando, Y.; Tanaka, T. Polyhedral Oligosilsesquioxane-Modified Boron Nitride Nanotube Based Epoxy Nanocomposites: An Ideal Dielectric Material with High Thermal Conductivity. *Adv. Funct. Mater.* **2013**, *23*, 1824–1831.
15. Kymäläinen, H.-R.; Sjöberg, A.-M. Flax and Hemp Fibres as Raw Materials for Thermal Insulations. *Build. Environ.* **2008**, *43*, 1261–1269.
16. Weidenfeller, B.; Höfer, M.; Schilling, F. R. Thermal Conductivity, Thermal Diffusivity, and Specific Heat Capacity of Particle Filled Polypropylene. *Composites, Part A* **2004**, *35*, 423–429.
17. Gelin, K.; Bodin, A.; Gatenholm, P.; Mihranyan, A.; Edwards, K.; Strømme, M. Characterization of Water in Bacterial Cellulose Using Dielectric Spectroscopy and Electron Microscopy. *Polymer* **2007**, *48*, 7623–7631.
18. Moon, R. J.; Martini, A.; Nairn, J.; Simonsen, J.; Youngblood, J. Cellulose Nanomaterials Review: Structure, Properties and Nanocomposites. *Chem. Soc. Rev.* **2011**, *40*, 3941–3994.
19. Coleman, J. N.; Lotya, M.; O'Neill, A.; Bergin, S. D.; King, P. J.; Khan, U.; Young, K.; Gaucher, A.; De, S.; Smith, R. J.; Shvets, I. V.; *et al.* Two-Dimensional Nanosheets Produced by Liquid Exfoliation of Layered Materials. *Science* **2011**, *331*, 568–571.
20. Siro, I.; Plackett, D. Microfibrillated Cellulose and New Nanocomposite Materials: A Review. *Cellulose* **2010**, *17*, 459–494.
21. Zhu, H.; Xiao, Z.; Liu, D.; Li, Y.; Weadock, N. J.; Huang, J.; Hu, L.; Fang, Z. Biodegradable Transparent Substrates for Flexible Organic-Light-Emitting Diodes. *Energy Environ. Sci.* **2013**, 2105–2111.
22. Huang, J.; Zhu, H.; Chen, Y.; Preston, C.; Rohrbach, K.; Cumings, J.; Hu, L. Highly Transparent and Flexible Nanopaper Transistors. *ACS Nano* **2013**, *7*, 2106–2113.
23. Lin, Y.; Williams, T. V.; Xu, T. B.; Cao, W.; Elsayed-Ali, H. E.; Connell, J. W. Aqueous Dispersions of Few-Layered and Monolayered Hexagonal Boron Nitride Nanosheets from Sonication-Assisted Hydrolysis: Critical Role of Water. *J. Phys. Chem. C* **2011**, *115*, 2679–2685.
24. Kemaloglu, S.; Ozkoc, G.; Aytac, A. Thermally Conductive Boron Nitride/SEBS/EVA Ternary Composites: "Processing and Characterization". *Polym. Compos.* **2010**, *31*, 1398–1408.
25. Gao, J. W.; Zheng, R. T.; Ohtani, H.; Zhu, D. S.; Chen, G. Experimental Investigation of Heat Conduction Mechanisms in Nanofluids. Clue on Clustering. *Nano Lett.* **2009**, *9*, 4128–4132.
26. Wang, J. J.; Zheng, R. T.; Gao, J. W.; Chen, G. Heat Conduction Mechanisms in Nanofluids and Suspensions. *Nano Today* **2012**, *7*, 124–136.
27. Wu, C. W.; Cho, T. J.; Xu, J. J.; Lee, D.; Yang, B.; Zachariah, M. R., Effect of Nanoparticle Clustering on the Effective Thermal Conductivity of Concentrated Silica Colloids. *Phys. Rev. E* **2010**, *81*.
28. Yang, B.; Chen, G. Partially Coherent Phonon Heat Conduction in Superlattices. *Phys. Rev. B* **2003**, *67* (011406), 1–4.
29. Kulachenko, A.; Denoyelle, T.; Galland, S.; Lindstrom, S. B. Elastic Properties of Cellulose Nanopaper. *Cellulose* **2012**, *19*, 793–807.
30. Iwamoto, S.; Kai, W. H.; Isogai, A.; Iwata, T. Elastic Modulus of Single Cellulose Microfibrils from Tunicate Measured by Atomic Force Microscopy. *Biomacromolecules* **2009**, *10*, 2571–2576.
31. Chen, S. S.; Moore, A. L.; Cai, W. W.; Suk, J. W.; An, J. H.; Mishra, C.; Amos, C.; Magnuson, C. W.; Kang, J. Y.; Shi, L.; *et al.* Raman Measurements of Thermal Transport in Suspended Monolayer Graphene of Variable Sizes in Vacuum and Gaseous Environments. *ACS Nano* **2011**, *5*, 321–328.
32. Carpenter, C.; Maroudas, D.; Ramasubramaniam, A. Mechanical Properties of Irradiated Single-Layer Graphene. *Appl. Phys. Lett.* **2013**, *103* (013102), 1–4.
33. Veca, L. M.; Meziani, M. J.; Wang, W.; Wang, X.; Lu, F. S.; Zhang, P. Y.; Lin, Y.; Fee, R.; Connell, J. W.; Sun, Y. P. Carbon Nanosheets for Polymeric Nanocomposites with High Thermal Conductivity. *Adv. Mater.* **2009**, *21*, 2088–2092.
34. Yang, B.; Liu, W. L.; Liu, J. L.; Wang, K. L.; Chen, G. Measurements of Anisotropic Thermoelectric Properties in Superlattices. *Appl. Phys. Lett.* **2002**, *81*, 3588–3590.
35. Yang, B.; Wang, P. *Thermoelectric Microcooler*; World Scientific Publishing Company, 2012.